

# Self-folding origami: shape memory composites activated by uniform heating

Michael T Tolley<sup>1,2</sup>, Samuel M Felton<sup>1</sup>, Shuhei Miyashita<sup>3</sup>, Daniel Aukes<sup>1</sup>, Daniela Rus<sup>3</sup> and Robert J Wood<sup>1,2</sup>

<sup>1</sup> School of Engineering and Applied Sciences, Harvard University, 60 Oxford Street, Cambridge, MA 02138, USA

<sup>2</sup> Wyss Institute for Biologically Inspired Engineering, Harvard University, 3 Blackfan Circle, Boston, MA 02115, USA

<sup>3</sup> Computer Science and Artificial Intelligence Laboratory, Massachusetts Institute of Technology, 32 Vassar St., Cambridge, MA 02139, USA

E-mail: [mtolley@seas.harvard.edu](mailto:mtolley@seas.harvard.edu), [dran@csail.mit.edu](mailto:dran@csail.mit.edu), [sam@seas.harvard.edu](mailto:sam@seas.harvard.edu), [shuheim@csail.mit.edu](mailto:shuheim@csail.mit.edu), [rus@csail.mit.edu](mailto:rus@csail.mit.edu) and [rjwood@seas.harvard.edu](mailto:rjwood@seas.harvard.edu)


Received 26 February 2014, revised 22 April 2014

Accepted for publication 24 April 2014

Published 11 August 2014

## Abstract

Self-folding is an approach used frequently in nature for the efficient fabrication of structures, but is seldom used in engineered systems. Here, self-folding origami are presented, which consist of shape memory composites that are activated with uniform heating in an oven. These composites are rapidly fabricated using inexpensive materials and tools. The folding mechanism based on the in-plane contraction of a sheet of shape memory polymer is modeled, and parameters for the design of composites that self-fold into target shapes are characterized. Four self-folding shapes are demonstrated: a cube, an icosahedron, a flower, and a Miura pattern; each of which is activated in an oven in less than 4 min. Self-sealing is also investigated using hot melt adhesive, and the resulting structures are found to bear up to twice the load of unsealed structures.

 Online supplementary data available from [stacks.iop.org/sms/23/094006/mmedia](http://stacks.iop.org/sms/23/094006/mmedia)

Keywords: self-folding, self-assembly, smart materials, shape memory polymers, origami, rapid fabrication

(Some figures may appear in colour only in the online journal)

## 1. Introduction

Engineered systems typically require complex, expensive, and time-consuming three dimensional (3D) fabrication processes for manufacturing, and require complicated infrastructures for assembly and/or deployment. Nature, on the other hand, is often able to rapidly fabricate lightweight structures using self-folding strings or sheets. Self-folding structures can be found in biology at length scales from nanometers to meters, such as organic molecules [1], winged insects [2], brains [3], and tree leaves [4, 5]. Self-folding automates the construction of arbitrarily complex geometries at arbitrarily large or small scales. Folding also has many advantages over traditional manufacturing methods, including

reduced material consumption and creation of structures with improved strength-to-weight ratios.

Folded designs have found useful engineering applications in areas such as space exploration [6] and logistics [7]. Complimentary theoretical work has proven that folding is in fact capable of achieving a large set of target geometries [8–10]. Recently, origami inspired folding has also enabled great strides in the fabrication of mm to cm scale robotics [11–13]. However, fold actuation remains a challenge as these robots often require many hours and/or microsurgeon dexterity to assemble manually. Reliable self-folding techniques would be a boon to automated fabrication of folded devices, as well as to self-deployable systems.

Research in small-scale fabrication has developed a variety of self-folding mechanisms. In one approach,

lithographically patterned thin films fold spontaneously via residual stress [14], while in another approach, hydrogel composites with differential swelling folded when exposed to water [15]. Layered composites have been shown to self-fold when exposed to a change in pH, temperature, or the addition of a solvent [16]. Self-folding mesoscale structures have been activated by lasers and magnetic fields [17, 18], and complex machines have been assembled via the Pop-Up Book MEMS technique [19, 20]. In focusing on how to fold structures too small to be directly manipulated in an accurate way, these previous approaches have employed expensive tools and materials, and in many cases used complex infrastructure for deployment (such as lasers and magnetic fields).

At the centimeter scale, we have previously used shape memory alloys to actuate a self-folding sheet of programmable matter [21]. In designing a universal sheet capable of folding into any shape, this approach relied on the use of complex materials and fabrication approaches, and would not be efficient in the assembly of specific target structures.

Recent work has employed selective light absorption with patterned inks to cause inexpensive, single-use shape memory polymers (SMPs) to self-fold into target structures [22, 23]. While this is a simple and inexpensive approach to self-folding, it faces a number of practical challenges. First, light-induced activation of self-folding is inherently directional, which can lead to occlusions during folding. Achieving uniform light intensity over large areas is an additional challenge. Furthermore, it is difficult to achieve well defined fold lines (i.e. sharp edges) using SMP alone. Finally, the use of the fold actuation material as the structural material limits the strength and potential applications of the structures formed.

We have recently demonstrated the use of similar SMPs, selectively actuated by resistive heaters, to realize self-folding robots and structures [24–26]. While this selective activation of SMPs for self-folding is powerful, it requires the inclusion of an electrical layer for the controlled electrical heating required for folding. For many applications, this additional complexity may be unnecessary and undesired.

Here we present an approach to the rapid, inexpensive fabrication of self-folding shape memory composites, or *self-folding origami*, which are activated with uniform heating (i.e. in an oven). We designed a process for the fabrication of shape memory composites consisting of three layers: a layer of SMP material sandwiched between two structural layers (with two additional adhesive layers bonding the laminate together). When placed into an oven, these composites fold into the desired structures automatically. We present models for predicting the geometry (i.e. angle) of a fold after actuation, and the overall torque applied by the SMP at a fold edge. We present experimental results demonstrating the folding of a variety of target structures (figure 1). We also present an approach to locking, or sealing, the self-folded structures.

## 2. Modeling

### 2.1. Fold angle model

Our self-folding laminates have built-in mechanical fold stops. The removal of a strip of the structural layer along the concave side of the fold lines frees the underlying SMP material to contract when heated (figure 2). In addition, the edges of this gap form mechanical stops which limit the fold angle. Consequently, it is possible to encode the fold angle in the design itself by adjusting the width of the gap at the hinges ( $w_{\text{gap}}$ ). From the geometry of the folded state (figure 2, right), we can find the following relation between the final fold angle,  $\theta$ , the thickness of the paper,  $t_{\text{paper}}$ , the thickness of the SMP after actuation,  $t'_{\text{SMP}}$ , and the distance  $\delta$  between the bottom of the SMP and the axis of rotation  $P$ . (Note that the laminates do not bend about the corner of the bottom layer due to compression in the paper, hence the distance  $\delta$ .)

$$\tan\left(\frac{\theta}{2}\right) = \frac{w_{\text{gap}}}{2(t_{\text{paper}} + t'_{\text{SMP}} + \delta)}. \quad (1)$$

### 2.2. Folding torque

The torque exerted by a self-folding hinge is dependent on the stress in the SMP due to the thermally induced activation ( $\sigma_x$ ), and the thickness of the SMP ( $t_{\text{SMP}}$ ), as well as the distance  $\delta$  between the SMP and the point of rotation  $P$  and the width  $W$  of the hinge (figure 2).

$$T = \sigma_x W t_{\text{SMP}} \left( \frac{t_{\text{SMP}}}{2} + \delta \right). \quad (2)$$

The stress along the length of the SMP ( $\sigma_x$ ) is first calculated by assuming that the SMP is constrained in the  $x$ - and  $y$ -directions, while undergoing no stress in the  $z$ -direction. When the SMP is activated, the  $x$  and  $y$  direction strains  $\epsilon_x$  and  $\epsilon_y$  are both equal to the activation strain  $\epsilon_a$ , and the material is not constrained in the  $z$  direction ( $\sigma_z = 0$ ). Thus, we can solve for the stress in terms of the activation stress  $\sigma_a$ :

$$\sigma_a = E\epsilon_a, \quad (3)$$

$$\epsilon_a = \epsilon_x = \epsilon_y. \quad (4)$$

For isotropic materials:

$$\epsilon_x = \frac{1}{E}(\sigma_x - \nu\sigma_y - \sigma_z), \quad (5)$$

$$\epsilon_y = \frac{1}{E}(\sigma_y - \nu\sigma_x - \sigma_z). \quad (6)$$

Thus,

$$\epsilon_a = \frac{\sigma_a}{E} = \frac{1}{E}(\sigma_x - \nu\sigma_y) = \frac{1}{E}(\sigma_y - \nu\sigma_x), \quad (7)$$

$$\sigma_a = (1 - \nu)\sigma_x. \quad (8)$$

Combining equations (2) and (8) results in our expression for torque:

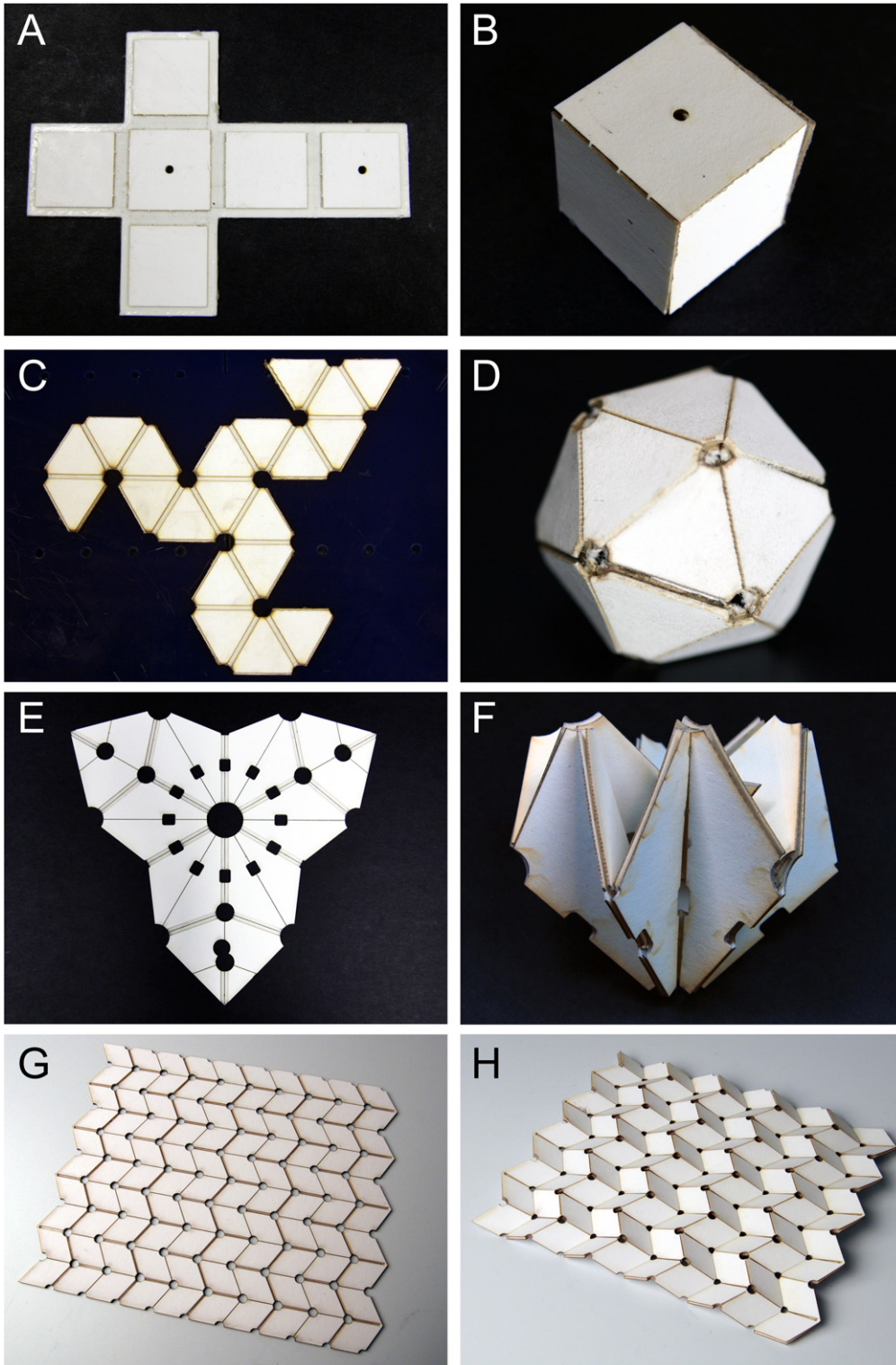


**Figure 1.** Self-folded geometries before (left) and after (right) activation in an oven at 130 °C. Each of these three-dimensional geometries, namely a cube (A, B), an icosahedron (C, D), a flower (E, F), and a Miura pattern (G, H), self-folded in an oven in under 4 min.

$$T = \frac{\sigma_a}{1 - \nu} W t_{\text{smp}} \left( \frac{t_{\text{smp}}}{2} + \delta \right). \quad (9)$$

The moment due to gravity, however, is due to the length  $L$  of the folding face and the mass  $m$  of the composite, which is composed of the mass of the SMP ( $m_{\text{smp}}$ ), and the mass of the

two layers of paper ( $m_{\text{paper}}$ ; we assume the mass of adhesive is negligible).

$$m_{\text{paper}} = 2WLt_{\text{paper}}\rho_{\text{paper}}, \quad (10)$$

$$m_{\text{smp}} = WLt_{\text{smp}}\rho_{\text{smp}}, \quad (11)$$

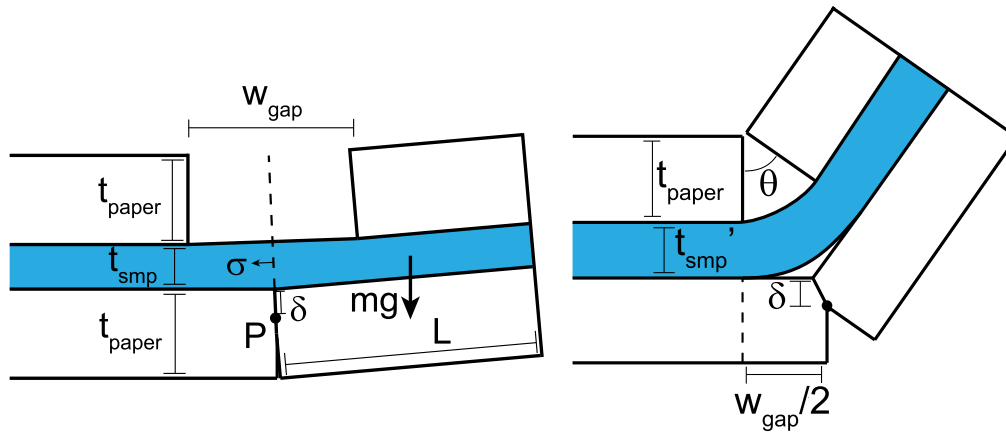


**Figure 2.** Schematic cross-section of a shape memory composite self-folding hinge. The shape memory composite consists of a layer of shape memory polymer (SMP, colored here in blue), with two patterned layers of paper (colored here in white). Left: when the laminate is activated with uniform heating, the SMP layer contracts, causing the laminate to bend towards the side with a gap about the perpendicular axis  $P$ , fighting against a moment caused by the force of gravity on the free end,  $mg$ . Right: the laminate continues bending until the two sides of the upper layer come into contact, resulting in a final bend angle  $\theta$ .

$$M = \frac{L}{2}mg = \frac{L}{2}(m_{\text{paper}} + m_{\text{smp}})g. \quad (12)$$

Here  $g$  is the acceleration of gravity of Earth. Because of these relationships, for any given composite, there is a maximum effective face length that can successfully self-fold (without design optimization for weight reduction, e.g. removal of unnecessary material). However, the width of the hinge is linearly related to both the torque and the moment, so a self-folding face can be arbitrarily wide.

### 3. Results and discussions

#### 3.1. Materials and fabrication

Our approach to the fabrication of self-folding shape memory composites is inspired by the ‘PC-MEMS’ and ‘Pop-up book MEMS’ techniques developed recently for the fabrication of microscale robotic systems [19, 20, 28]. However, there are a number of key differences in our approach. First, we limited ourselves to the use of inexpensive, readily available materials and tools. Second, inspired by origami, we chose to use a single mechanical layer (sheet) to achieve complex 3D shapes with multiple folds following different degrees of freedom (as opposed to ‘pop-up’ devices which are complex parallel linkages connected to a single degree of freedom). Third, the use of a heat-activated SMP layer precludes the use of solid sheet adhesives used to achieve the ‘mechanical vias’ in previous complex pop-up designs [19]. This is because the SMP layer would be prematurely activated while setting the adhesive. Otherwise, a solid adhesive with an activation temperature lower than that of the SMP would likely lose adhesive strength during activation of the SMP. Thus, we are limited to liquid adhesives or two-sided tapes.

Taking the constraints mentioned above into account, we designed a process for the fabrication of shape memory composites consisting of three layers: a layer of our SMP

material sandwiched between two structural layers, with two additional adhesive layers holding the laminate together (figure 3) [29].

For the SMP layer we used prestrained polystyrene shrink film sheets (commercially available as the children’s toy, Shrinky Dinks), which have previously been used in the fabrication of microfluidic molds [30], and folded structures activated with light [22]. These sheets contract isotropically to  $\sim 50\%$  of their initial size when heated above their activation temperature of  $\sim 107^\circ\text{C}$ . These sheets are inexpensive, and easily patterned on a  $\text{CO}_2$  laser machining system. For the structural layers we used  $508\ \mu\text{m}$  (20 mil) thick paper (also known as paperboard).

We bonded the three layers together with double-sided, 50 mm thick silicone tape (ARclad 7876, Adhesives Research). We tested many double-sided tapes (mostly acrylic-based) and only silicone tape maintained adhesion at the elevated temperatures required to activate the SMP.

To fabricate the self-folding composites, we predefined the fold patterns on the paper and SMP layers using a  $\text{CO}_2$  laser machining system (VLS 2.3, Universal Laser Systems; figures 3(A)–(C)). Connections at the end of each fold edge held the faces of the composite in place after laser machining. We stacked the three layers, using alignment pins, and dispensed a layer of the silicone tape in between each for adhesion (figure 3(D)). A final cut consisting of a circle at the end of each fold line (figure 3(E)) then released the self-folding composite from the surrounding supporting structure (figure 3(F)). The faces of the flower shape were additionally connected with tabs at the center of the long edges which were cut with rectangular release cuts (figure 1(E)).

#### 3.2. Fold angle characterization

To characterize the fold angle as a function of the actuator geometry, we built self-folding test strips with gaps on the inner layer in the range of 0.25–12 mm (some of these strips are shown in figure 4). We activated these strips in an oven at

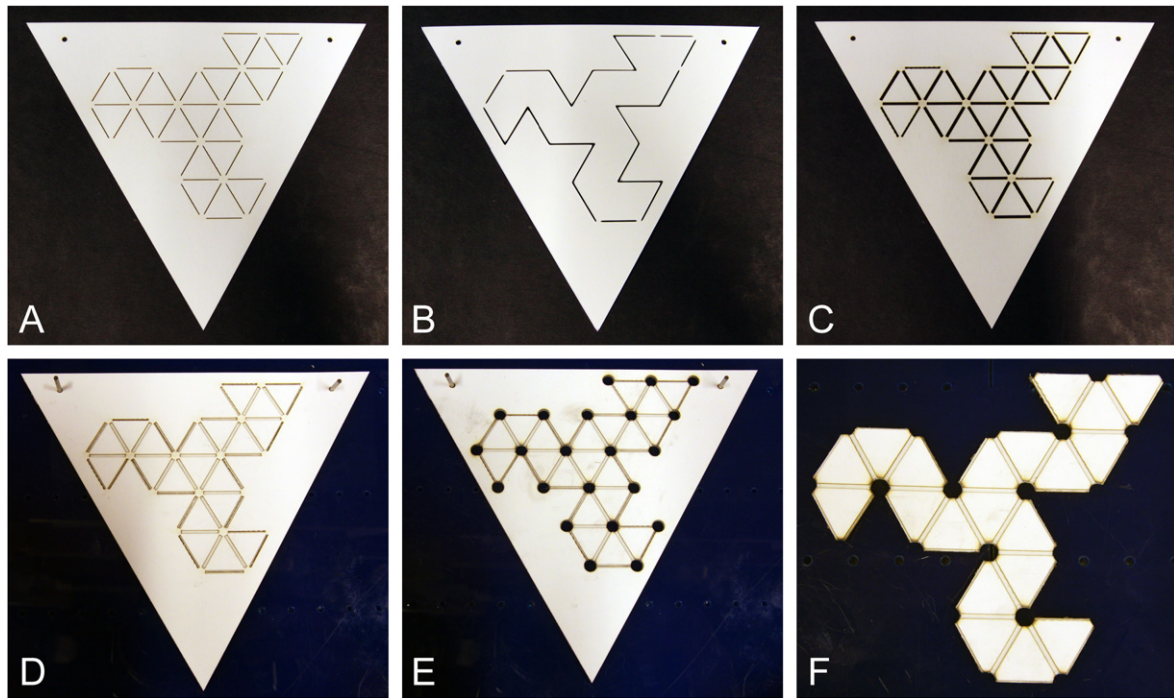


**Figure 3.** Self-folding laminate fabrication. Three layers patterned with a CO<sub>2</sub> laser machining system make up a self-folding laminate: (A) a lower structural paperboard layer, (B) a shape memory polymer layer, and (C) an upper structural paperboard layer. (D) These layers are aligned on pins and adhered together with double-sided silicone tape. (E) A final release cut removes the support structure, leaving only (F) the shape memory laminate.

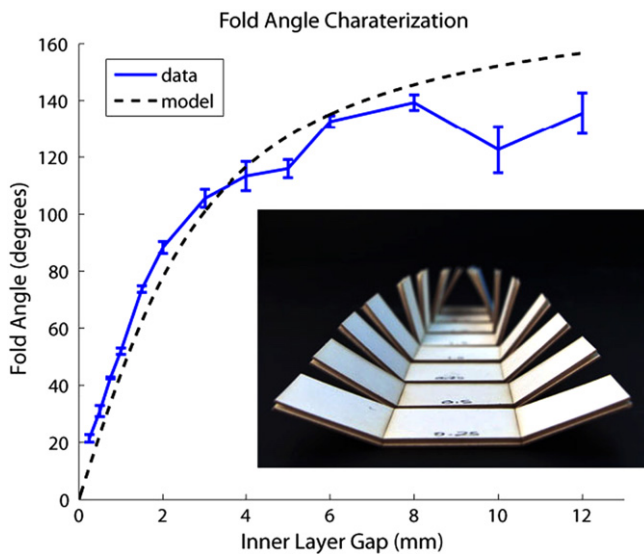


**Figure 4.** Experimental characterization of the final fold angle of a self-folding shape memory composite fold as a function of the patterned inner gap layer. Error bars indicate the standard deviation in the measured final angle from experiments consisting of four samples per gap width. Our experimental results showed close correlation with the geometric model presented in section 2.1 up to a fold angle of approximately 130°. Inset: Actuated test pieces with two folds each and gap widths,  $w_{gap}$ , ranging from 0.25 mm to 4 mm.

130 °C. For each gap width, we fabricated four test folds. After activation, we measured the angle of each fold.

Figure 4 shows the average and standard error of the final fold angle corresponding to each  $w_g$  ( $n = 4$ ). The geometric

model presented in section 2.1 is also plotted for comparison. We found close agreement between the model and experimental results up to a gap width of 8 mm corresponding to a fold angle of 139°. After this point, contraction of the SMP layer was not sufficient to bring the two edges of the gap together as modeled in figure 2. Nonetheless, for angles less than 139°, these results supported the use of the model in the subsequent design of self-folding shape memory composites.

### 3.3. Folding torque characterization

We created 30 mm wide test hinges of varying length in order to characterize the folding torque of the self-folding composite. One side of these hinges was held flat in the oven, while the other was allowed to move freely during folding. The lengths of the moving faces on these test hinges varied from 60 to 220 mm. The final angles are plotted in figure 5. These data are compared to the calculated moment exerted on these self-folding hinges due to gravity, as well as the calculated torque exerted by the hinges. In calculating the torque, we assumed the Poisson ratio of the SMP in its activated rubbery state,  $\nu$ , to be 0.5 [27].

We expected that the hinges which had a folding torque greater than the resisting moment would fold completely to a final angle of approximately 45°, while those with insufficient torque to overcome gravity would remain at 0°. Instead, as the face length approached the crossover point, the final angle slowly decreased, until it fell rapidly at the crossover point. We believe this discrepancy is due to the viscoelastic properties of the SMP in its rubber state, allowing for plastic

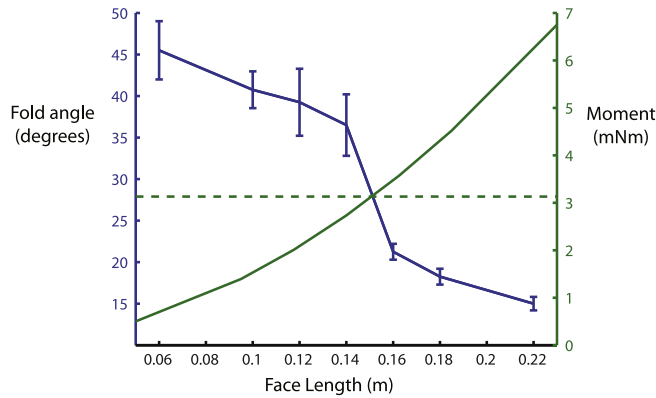


**Figure 5.** A plot of measured final fold angle (blue) of test hinges with varying face lengths, compared to a graph of the modeled moment (green) due to gravity on the face that is resisting the folding torque. The dashed line indicates the torque exerted by each test hinge, and the length at which the dashed and solid green lines cross indicates the expected maximum face length that can still be folded. For the fold angle data, error bars indicate the standard deviation in the measured angle for experiments consisting of four samples per face length.

deformation due to the resisting moment. SMPs typically behave elastically during their rubber state due to entanglement of their constituent polymer chains with direct neighbors; however, prolonged external stress results in slipping and disentangling of the polymer chains into new energetically favorable positions, resulting in plastic deformation [31].

For hinges with faces longer than 150 mm, we expected no folding, but measured minor angular deflections of at least 15°. We believe that this is due to residual stress in the activated SMP after cooling; during activation, these samples remained flat, but once cooled and removed from the oven, they stiffened and exhibited minor deflections. We also saw a gradual decrease in the angle of these deflections, which can be explained as before by plastic deformation proportional to the applied stress.

We determined the activation stress of the PPS by measuring and averaging the contractile force of five dogbone samples of the material in a universal mechanical testing machine (5544A, Instron). The strips were 10 mm wide at their thinnest points, and force was measured as the samples were heated with a heat gun to their transition temperature. We assume that at some point during the measurement the PPS has uniformly transitioned to its rubber state, but has not yet plastically deformed. We measured the activation stress under uniaxial loading. Since the material was not constrained in the  $y$  direction for these tests, the transverse stress,  $\sigma_y$  is 0, thus we can calculate the activation stress with the relationship  $\sigma_a = \sigma_x = F_x/A$ . Based on these measurements, we found the activation stress of the PPS to be 696 kPa.

### 3.4. Self-folding origami design

Using the results of our fold angle characterization (see section 3.3), we designed and tested four self-folding origami

shapes: a cube, an icosahedron, a flower, and a Miura pattern (figure 1). These self-folding laminates were designed using either commercially available 2D CAD software (for the cube, icosahedron, and Miura pattern), or a custom CAD tool under development called popuCAD [32] (for the flower).

The five folds comprising the cube shape are 90° each. Thus, based on our characterization, we used a gap width of 2 mm. The largest moment that an actuated edge of the cube must fold against is the initial moment due to two flat faces (see figure 1(A)). Based on this, our torque model predicts a maximum cube length of 75 mm. However, experimentally we observed that outer edges (which have less mass to lift), tend to fold first, which decreases the moment due to gravity exerted on the inner edges (due to a decrease of the lever arm as outer faces fold). On the other hand, we observed a drop in the fold angle for strips longer than 60 mm, which would limit the maximum cube length to 30 mm. Incorporating a factor of safety we used 20 mm edges.

A regular icosahedron has a dihedral angle of 138.2°. Thus, the 19 actuated folds of our icosahedron design required a fold angle of 41.8°, corresponding to an internal gap width of 0.73 mm (we used 0.75 mm). For the icosahedron net shown in figure 1(C), in the worst case scenario a single edge of width  $w$  must lift seven faces of area  $\sqrt{3}w^2/4$  each, with an overall centroid of a distance  $10\sqrt{3}w/21$  perpendicular from the edge, resulting in a moment due to gravity of:

$$M = \frac{35g \left( 2t_{\text{paper}}\rho_{\text{paper}} + t_{\text{smp}}\rho_{\text{smp}} \right) w^3}{2}. \quad (13)$$

Comparing this case with our torque model for a strip of self-folding composite, the moment experienced in this case (as a function of the icosahedron face width  $w$ ) is a factor of  $\sqrt{35}$  larger. Thus, the theoretical maximum self-foldable icosahedron face length is 25 mm (again, ignoring any reduction in this moment due to the folding outer faces). Adding a factor of safety, we chose to use a face length of 15 mm.

For the flower design, we used a gap width of 4 mm at every actuated fold, corresponding to a maximum fold angle of 110°. However, unlike in our test strips or cube and icosahedron designs, the parallel nature of the folds in the flower design led to a complicated relationship between the gap widths and resulting fold angles. We leave an in-depth analysis of this relationship to future work. For the Miura pattern, we used a gap width of 1 mm for every fold.

### 3.5. Self-folding experiments

We tested each of the self-folding composites by activating them in an oven preheated to  $\sim 130^\circ\text{C}$ . The laminates were placed on preheated ceramic tiles to heat them as evenly as possible. Figure 6 shows frames from each of these experiments with the time elapsed since being inserted into the oven indicated on each frame. After an initial heating period of 15–30 s, the laminates began folding, completing the target structure in 1–4 min (larger designs took more time to

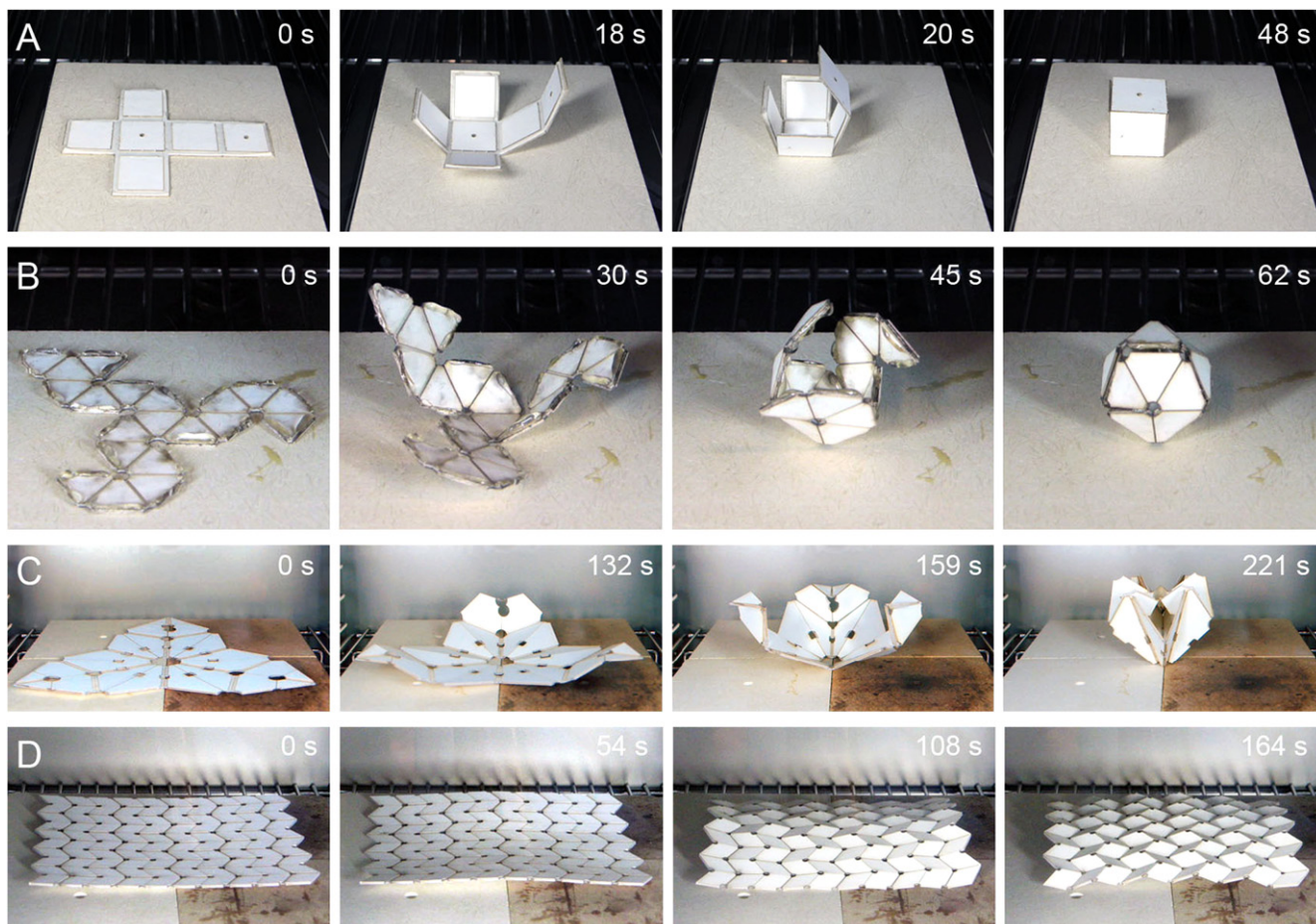


**Figure 6.** Self-folding experiments. These image sequences are from self-folding experiments for the cube (A), icosahedron (B), and Miura pattern (D) shapes (see also Movie S1). In each case, the self-folding shape memory composite was inserted into an oven preheated to 130 °C. The time elapsed since the start of the experiment is indicated in the lower-right corner of each frame.

**Table 1.** Experimental self-folded geometries.

Geometry	Faces	Actuated edges	Maximum dimension (folded)
Cube	6	5	15 mm
Icosahedron	20	19	25 mm
Flower	24	30	70 mm
Miura Pattern	100	180	150 mm

complete folding). At this point, the structures were removed from the oven. While the activated SMP still exhibited compliance at the activation temperature, it quickly solidified as it cooled, resulting in a rigid structure. The number of faces, actuated folds, and overall dimensions of each test geometry are summarized in table 1.

The four self-folding origami geometries folded successfully when activated in the oven. However, we observed variability in shapes consisting of many serial folds (e.g. the icosahedron). This can be explained by variability in the final fold angle of single edges due to manufacturing limitations (see figure 4). In such shapes, fold angle errors can integrate, resulting in misalignment in the final structure (see, for e.g.,

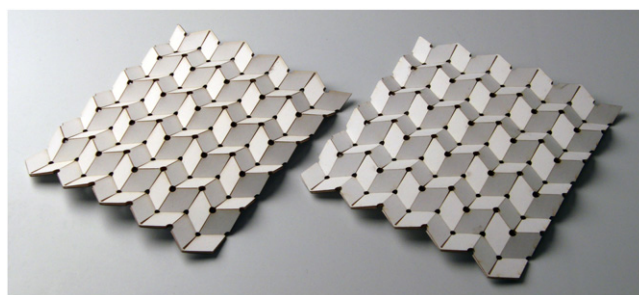


**Figure 7.** Repeatability of folding. Fabrication limitations inhibited the repeatable self-folding of large structures with many sequential folds working against gravity. However, self-folding repeatability was improved for structures with many folds acting in parallel, such as the two copies of the same Miura pattern seen here.

figure 8(B)). Larger structures were also more affected by gravity, as predicted and observed in our folding torque model and characterization (respectively).

To counteract both of these sources of variability, we designed structures with multiple actuated folds working in parallel. For example, the flower pattern (figures 1(C) and 6(C)) had symmetric ‘petals’ with multiple folds working

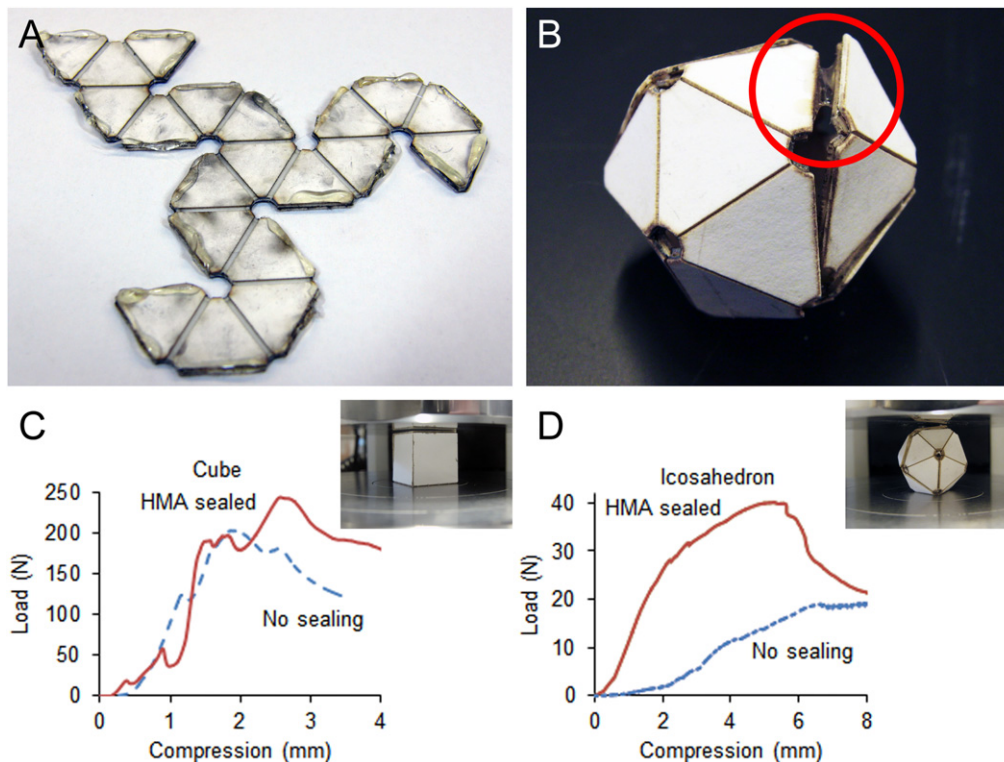


**Figure 8.** Sealing with hot melt adhesive. (A) Hot melt adhesive is patterned around the edges of the self-folding laminate prior to activation in an oven. (B) A self-folded icosahedron. A glue bridge (circled) formed between two edges is visible because of misalignment. (C) Strength testing shows the increased load carrying capacity of sealed cube and (D) icosahedron shapes.

together to form the final shape. The result was a diminished effect of gravity and an improved repeatability of the final fold angles.

Similarly, the Miura pattern nominally has only a single degree of freedom, and in theory it could be folded with a single (sufficiently strong) actuator. However, since we actuated every edge, and actuated edges worked in parallel to determine fold angles, fold angle errors tended to cancel one another, resulting in a regular and repeatable final structure (figure 7).

### 3.6. Sealing with hot melt adhesive (HMA)

We investigated the possibility of achieving both self-folding and self-sealing structures with the use of HMA. HMAs, commonly used in ‘glue guns’, melt at temperatures in the range of 120 °C–193 °C. Thus, lower melting point HMAs can be activated at the same temperature as our self-folding composites (130 °C) in order to seal the edges of structure during self-folding.

We manually deposited HMA onto the edges of our self-folding cube and icosahedron composites (figure 8(A)). These shapes folded as before, except the glue added some resistance to folding that led to incomplete folds (figure 8(B)). This increased resistance was overcome by increasing the gap widths of the laminate cut pattern, increasing the ‘desired’ fold angle according to the relationship described in section 3.3 by approximately 10°.

We compared the strength of sealed and unsealed self-folded structures on the universal mechanical testing machine

by subjecting them to compressive testing. The loads borne by the sealed and unsealed cube and icosahedron are plotted versus compression in figures 8(C) and (D), respectively. While the failure mode of these folded structures in compression is complex, it is apparent that sealing did increase the strength of each structure.

## 4. Conclusions

We have presented self-folding origami composed of shape memory composites which are activated with uniform heating in an oven. These composites can be rapidly fabricated using inexpensive materials and tools. We have modeled the folding mechanism and characterized parameters for the design of composites that self-fold into target shapes. We demonstrated this process with four shapes, and discovered that shapes with folds that act in parallel (such as the flower and Miura pattern) exhibit less variability in self-folding than shapes with many serial folds (such as the icosahedron). We additionally presented an approach to the self-sealing of these laminates using HMA.

This work represents a first step in a new fabrication paradigm. Many opportunities for future work exist, including the development of improved software tools for self-folding origami design, to which traditional CAD software is not particularly well suited. Otherwise, future work could investigate the automatic generation of 2D composite designs to achieve a desired 3D shape [33], a reduction in the variability



in folded structures through improvements in composite design or fabrication, or increasing the functionality of the folded structures by adding additional layers for post-folding actuation, sensing, or communication.

## Acknowledgments

The authors would like to thank Daniel Sanchez for his assistance with fabrication which contributed to this work. The authors would also like to gratefully acknowledge support from the National Science Foundation (award numbers CCF-1138967 and EFRI-1240383). Any opinions, findings and conclusions or recommendations expressed in this material are those of the authors and do not necessarily reflect those of the National Science Foundation.

## References

- [1] Kellermayer M S Z, Smith S B, Granzier H L and Bustamante C 1997 Folding-unfolding transitions in single titin molecules characterized with laser tweezers *Science* **276** 1112–6
- [2] Haas F and Wootton R J 1996 Two basic mechanisms in insect wing folding *Proc. R. Soc. B* **263** 1651–8
- [3] Todd P 1982 A geometric model for the cortical folding pattern of simple folded brains *J. Theor. Biol.* **97** 529–38
- [4] Eisner T 1981 Leaf folding in a sensitive plant: a defensive thorn-exposure mechanism? *Proc. Natl. Acad. Sci.* **78** 402–4
- [5] Kobayashi H, Kresling B and Vincent J F 1998 The geometry of unfolding tree leaves *Proc. R. Soc. B* **265** 147–54
- [6] Miura K 1985 Method of packaging and deployment of large membranes in space *Inst. Space Astronautical Rep.* **618** 1–9
- [7] Konings R and Thijs R 2001 Foldable containers: a new perspective on reducing container-repositioning costs *Eur. J. Transp. Infrastruct. Res.* **1** 333–52
- [8] Benbernou N, Demaine E D, Demaine M L and Ovadya A 2011 Universal hinge patterns for folding orthogonal shapes origami 5: *Fifth Int. Meeting of Origami Science, Math, and Education* p 405
- [9] Demaine E D, Demaine M L and Mitchell J S B 2000 Folding flat silhouettes and wrapping polyhedral packages: new results in computational origami *Comput. Geom.* **16** 3–21
- [10] Demaine E D and Demaine M L 2001 Recent results in computational origami *Proc. of the 3rd Int. Meeting of Origami Science, Math, and Education* pp 3–16
- [11] Onal C D, Wood R J and Rus D 2011 Towards printable robotics: origami-inspired planar fabrication of three-dimensional mechanisms *IEEE Int. Conf. on Robotics and Automation (ICRA)* pp 4608–13
- [12] Onal C D, Wood R J and Rus D 2012 An origami-inspired approach to worm robots *IEEE/ASME Trans. Mechatronics* **18** 430–8
- [13] Wood R J 2008 The first takeoff of a biologically inspired at-scale robotic insect *IEEE Trans. Robot.* **24** 341–7
- [14] Bassik N, Stern G M and Gracias D H 2009 Microassembly based on hands free origami with bidirectional curvature *Appl. Phys. Lett.* **95** 091901
- [15] Guan J, He H, Hansford D J and Lee L J 2005 Self-folding of three-dimensional hydrogel microstructures *J. Phys. Chem. B* **109** 23134–7
- [16] Ionov L 2011 Soft microorigami: self-folding polymer films *Soft Matter* **7** 6786–91
- [17] Judy J W and Muller R S 1997 Magnetically actuated, addressable microstructures *J. Microelectromech. Syst.* **6** 249–56
- [18] Yi Y W and Liu C 1999 Magnetic actuation of hinged microstructures *J. Microelectromech. Syst.* **8** 10–17
- [19] Sreetharan P, Whitney J, Strauss M and Wood R 2012 Monolithic fabrication of millimeter-scale machines *J. Micromech. Microeng.* **22** 055027
- [20] Whitney J, Sreetharan P, Ma K and Wood R 2011 Pop-up book mems *J. Micromech. Microeng.* **21** 115021
- [21] Hawkes E, An B, Benbernou N M, Tanaka H, Kim S, Demaine E D, Rus D and Wood R J 2010 Programmable matter by folding *Proc. Natl. Acad. Sci.* **107** 12441–5
- [22] Liu Y, Boyles J K, Genzer J and Dickey M D 2012 Self-folding of polymer sheets using local light absorption *Soft Matter* **8** 1764–9
- [23] Liu Y, Mailen R, Zhu Y, Dickey M D and Genzer J 2014 Simple geometric model to describe self-folding of polymer sheets *Phys. Rev. E* **89** 042601
- [24] Felton S M, Tolley M T, Onal C D, Rus D and Wood R J 2013 Robot self-assembly by folding: a printed inchworm robot *IEEE Int. Conf. on Robotics and Automation (ICRA)* pp 277–82
- [25] Felton S M, Tolley M T, Shin B, Onal C D, Demaine E D, Rus D and Wood R J 2013 Self-folding with shape memory composites *Soft Matter* **9** 7688–94
- [26] Tolley M T, Felton S M, Miyashita S, Xu L, Shin B, Zhou M, Rus D and Wood R J 2013 Self-folding shape memory laminates for automated fabrication *IEEE/RSJ Int. Conf. on Intelligent Robots and Systems (IROS)* pp 4931–6
- [27] Mott P, Dorgan J and Roland C 2008 The bulk modulus and poisson's ratio of 'incompressible' materials *J. Sound Vib.* **312** 572–5
- [28] Ma K Y, Chirarattananon P, Fuller S B and Wood R J 2013 Controlled flight of a biologically inspired, insect-scale robot *Science* **340** 603–7
- [29] Miyashita S, Onal C D and Rus D 2013 Self-pop-up cylindrical structure by global heating *IEEE/RSJ Int. Conf. on Intelligent Robots and Systems (IROS)* pp 1466–73
- [30] Chen C S, Breslauer D N, Luna J I, Grimes A, Chin W, Lee L P and Khine M 2008 Shrinky-dink microfluidics: 3D polystyrene chips *Lab Chip* **8** 622–4
- [31] Lendlein A and Kelch S 2002 Shape-memory polymers *Angew. Chem. Int. Ed.* **41** 2034–57
- [32] Aukes D M, Goldberg B, Cutkosky M R and Wood R J 2014 An analytic framework for developing inherently-manufacturable pop-up laminate devices *Smart Mater. Struct.* **23** 094013
- [33] An B, Miyashita S, Tolley M T, Aukes D M, Meeker L, Demaine E D, Demaine M L, Wood R J and Rus D 2014 An end-to-end approach to making self-folded 3D surface shapes by uniform heating *IEEE/RSJ Int. Conf. on Intelligent Robots and Systems (IROS)*